Acta Geologica Polonica, Vol. 58 (2008), No. 1, pp. 13-26

Pleistocene neotectonics and Fe-mineralizations in the Ahnet-Mouydir area (northern margin of the Hoggar Massif, Algerian Sahara)

JOBST WENDT, UDO NEUMANN & HARTMUT SCHULZ

Institut für Geowissenschaften der Universität, Sigwartstrasse 10, D 72076 Tübingen, Germany.
E-mails: jobst.wendt@uni-tuebingen.de, udo.neumann@uni-tuebingen.de,
hartmut.schulz@uni-tuebingen.de

ABSTRACT:

WENDT, J., NEUMANN, U. & SCHULZ, H. 2008. Pleistocene neotectonics and Fe-mineralizations in the Ahnet-Mouydir area (northern margin of the Hoggar Massif, Algerian Sahara). *Acta Geologica Polonica*, **58** (1), 13-26. Warszawa.

Strongly mineralized lithologies were found in 4 different depositional settings along the northern margin of the Hoggar Massif in southern Algeria: (1) Pleistocene fluvial terraces, (2) pebble-filled erosional furrows in marine Silurian and Upper Devonian shales, (3) sedimentary dykes in Givetian mud buildups and (4) tectonic fault-fissures and cracks in Upper Devonian shales. In spite of the contrasting sedimentary environment, all these rocks display very similar properties and are considered as contemporaneous. They are characterized by high porosities, intense Fe-mineralization and a great variety of accompanying, secondary minerals formed in a sub-recent continental regime under pluvial to arid conditions. The dykes, faults and cracks are direct evidence of tensional stress during the early and middle Pleistocene which has not been observed so far. The complex sedimentary and diagenetic history of conglomerates, breccias, sandstones, ferricretes, calcretes and claystones in these settings was analyzed using SEM, EDX-microprobe, XRD, transmitted and reflected light petrography and is documented in hitherto unknown details.

Key words: Algeria, Hoggar, Pleistocene, Neotectonics, Terraces, Sedimentary dykes, Mineral composition, Diagenesis.

INTRODUCTION

Evidence of young intracratonic deformation on the stable margin of the West African Craton has occasionally been reported, but was mostly revealed only from seismic lines or satellite images. Such a large- or mega-scale observation can hardly be adopted in the field where indications of neotectonic activity are so limited that they generally escape attention. However, the desert climate and the concomitant absence of vegetation in the Algerian Sahara facilitate the direct identification of minute tectonic features which in a regional context can be related to larger-scale movements. In this contribution we describe the widespread mineralized terraces of early to middle Pleistocene age and the hitherto unknown occurrence of similar and coeval lithologies in tectonically induced dykes, faults and cracks. In addition, a survey is presented of the complex diagenetic history of the mineralized rocks and their relation to the climatic evolution of this part of the Sahara during the Pleistocene.

GEOLOGICAL SETTING

The Hoggar Massif is part of the West African Shield which was cratonized during several orogenic phases between 2000 and 700 Ma (BERTRAND & *al*. 1983). Precambrian metamorphics and Lower Cambrian granites are overlain by an up to 5 km thick pile of Upper Cambrian to Upper Carboniferous conglomerates, sandstones, shales and carbonates (BEUF & *al*. 1971, FABRE 1976). Lower Palaeozoic rocks are exclusively siliciclastic, deposited on a wide shelf in fluvial, deltaic and shallow marine environments. A deeper marine interval occurred during the Early Silurian documented by black graptolite shales ("hot shales") which constitute the main source rock of the North African hydrocarbon reservoirs (LÜNING & *al*. 2000). During the late Early Devonian a basin-and-ridge morphology was established, probably induced by reactivation of ancient (Precambrian) lineaments. Simultaneously with a sea-level highstand in the early Givetian, spectacular mud buildups formed on top and along the flanks of the ridges (WENDT & *al*. 2006). The Upper Devonian is characterized by a monotonous playa-sedimentation which is interrupted by two minor transgressions. The Carboniferous is represented by three transgressive-regressive cycles which display a very heterogeneous pattern of siliciclastics and limestones. The sea retreated from the area in the late Late Carboniferous (J. CONRAD 1984). The Variscan deformation during the latest Carboniferous/earliest Permian was relatively weak along the northern margin of the Hoggar Massif and is characterized by broad N-S running folds as well as by normal and reverse faults (J. CONRAD 1984). Apart from a few continental deposits (so-called "Continental Intercalaire") and intrusion of doleritic dykes of Middle Jurassic age, the entire area was peneplained and deeply eroded until the renewed flooding during the late Cenomanian. After the final regression of the sea during the Eocene, discontinuous continental deposits covered the area during the Neogene, accompanied by erosional activity under oscillating climatic conditions. The Pleistocene climate of the northern and central Sahara is characterized by four main humid-pluvial and four arid phases (MONOD 1964, ROGNON 1967b, G. CONRAD 1970, BAUMHAUER & *al*. 1989, ROGNON 1989). These major climatic cycles are superimposed by minor oscillations reflecting shorter-term monsoon variability, as has been revealed from the input of aeolian dust into marine sediments of the Mediterranean (LARRASOANA & *al*. 2003). The Precambrian Hoggar Massif was affected by strong volcanic activity during the late Miocene, Plio- and Pleistocene which still nowadays shows weak repercussions (ROGNON 1967a, GIROD 1971).

PREVIOUS WORK

The term neotectonics is generally applied to post-Miocene movements which have affected only the uppermost parts of the earth's crust and are related to seismic or aseismic activities (HANCOCK 1994). Some authors have used the same term for all tectonic movements on the West African Craton postdating the Variscan deformation at the Carboniferous/Permian transition. Post-Variscan intraplate tectonics is widely documented on the West African Craton and can be referred to six major periods (GUIRAUD & *al*. 1987): Early/Middle Jurassic, Aptian, Santonian, end Cretaceous, late Eocene and Miocene. The earliest movements are expressed by a network of doleritic dykes which manifest the widespread Middle Jurassic volcanism in the Reggane and Tindouf Basins (J. CONRAD 1972, 1981; SMITH & *al*. 2006). Local weak folds of presumed Early Cretaceous age are capped by the late Cenomanian transgression (FABRE 1976). An "important tectonic phase" is assumed to have taken place prior to the Eocene transgression (BIROT & *al*. 1955, FOLLOT 1953), but apart from this general statement, detailed observations are lacking.

The uplift of the Hoggar Massif since the Eocene and the onset of the basaltic (locally intermediate and acidic) volcanism in the late Miocene were accompanied by tectonic movements which partly follow Precambrian lineaments (FOLLOT 1953, GIROD 1971). ROGNON (1967a, p. 434) distinguished three main phases of deformation which, however, have not been calibrated. Some of these young N-S running fractures can be followed for 20-25 km. One of the most conspicuous is the Amguid fault in the eastern Mouydir (BIROT & DRESCH 1955) which bounds the Neogene-Quaternary depression of Amguid to the east. An attempt to correlate the sedimentological and morphological evolution on the northern margin of the Hoggar Massif since the late Late Cretaceous with these poorly defined neotectonic movements was presented by G. CONRAD (1970, p. 438). On the basis of geomorphological features, G. and J. CONRAD (1982) have argued that the early and middle Pleistocene was a period of tectonic activity in the Ahnet-Mouydir, but did not contribute any data. Other recent deformations, partly reactivating earlier structures, were revealed by analyses of satellite images in the area west and northwest of the Hoggar Massif (CHOROWICZ & FABRE 1997).

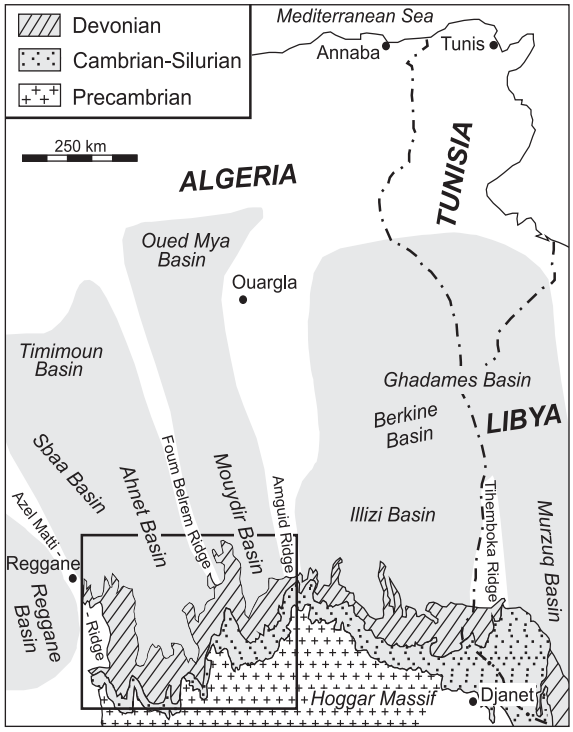

Fig. 1. Location of the study area in the framework of North African basins and ridges. Boxed area shows field of Text-fig. 2 (modified from WENDT & *al*. 2006)

MATERIAL AND METHODS

The material for the present study was collected from 43 localities of Silurian and Devonian deposits in the Ahnet and Mouydir regions (see appendix and Text-figs 1, 2). Most specimens were first thin-sectioned and became transparent only at about 0.01 mm thickness, but did not show many structural details within the opaque portions of the rock. Polished sections, however, yield very precise information about the mineral phases, the porosity and the microstructure. For the petrographic examination a Leica Laborlux 12 Pol S microscope with transmitted- and reflected-light was used. Mineral identification and most observations of fine-grained samples were performed using an oil immersion objective (20x/0.40). X-ray diffraction analyses were performed at our laboratory in Tübingen using a BRUKER D8-GADDS micro-diffractometer with a CoKα - XRay-tube (at 30kV/30mA) with graphite primary-monochromator, X-ray-lens with 50 micrometer spotsize (here app. 400 µm caused by rotating of the sample and 10° incident angle), Eulerian cradle with x-y-z-stage and sample rotation, and a GADDS-2D-detector system.

Samples analyzed under the scanning electron mi-

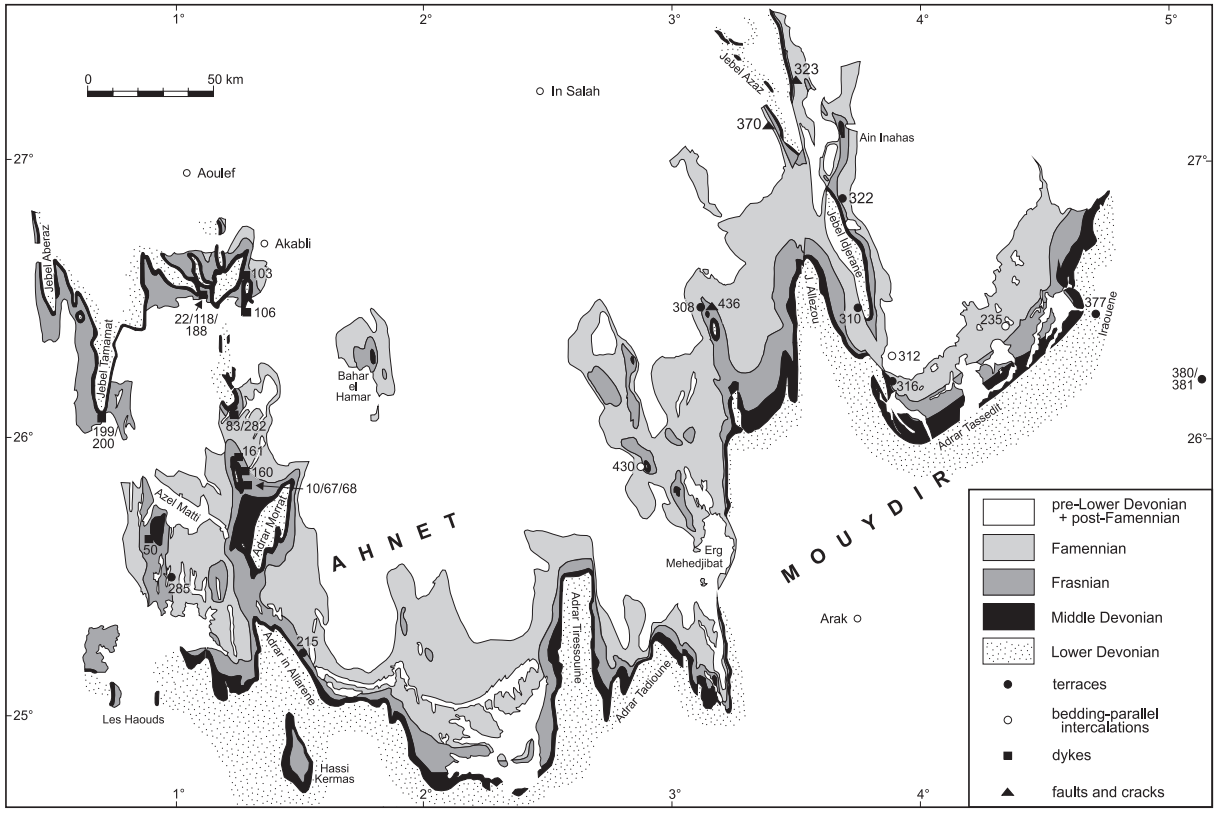

Fig. 2. Simplified geological map of the Ahnet-Mouydir area with sample localities (modified from WENDT & *al*. 2006)

croscope (SEM) have been mounted on conventional aluminium SEM-stubs and coated with carbon. SEM and backscatter electron pictures were taken prior to energy-dispersive X-ray analysis (EDX). A LEO VP 1450 SEM was operated at 15 kV EHT/2.575A at a working distance of 15 mm. The elemental composition of the polished sample surfaces was determined using a LINK Pentafet Si(Li)-drifted detector crystal (Oxford Instruments System INCA 200) at measuring times between 60 and 120 seconds. We concentrated on the elements O, Mg, Al, Si, P, S, Cl, Ca, Mn and Fe expressed here as atomic weight % using the strobe peak function and the XPP correction model for quantification.

DEPOSITIONAL ENVIRONMENT AND MINERALOGY

Four types of occurrence of mineralized lithologies and their relation to the underlying or host rocks can be distinguished (Table 1):

Fluvial terraces

In the study area they are best developed in the Iraouene Mountains of the eastern Mouydir (Text-fig. 2) where they overlie black, greyish or reddish weathering shales of the Lower Silurian Imirhou Formation (Pl. 1, Figs 1, 2). Among the three fluvial terraces which were morphologically distinguished by FOLLOT (1952) and G. CONRAD (1970), the upper and the middle one are most conspicuous. Generally both terraces are heavily mineralized by iron oxides and hydroxides ("cuirassé" in the French terminology). Morphologically less prominent remnants of mineralized terraces are preserved in other places of the Ahnet-Mouydir where they overlie Upper Devonian sandstones (Grès de Mehden Yahia) and shales (Argiles de Temertasset). Due to the profuse Fe-mineralization, the specific weight of individual samples is between 3.2 and 3.5. Thickness of the conglomeratic layers ranges from about 1 to 5 m. They alternate with middle- to coarse-grained ferruginous sandstones which often exhibit high-angle cross-bedding. Due to their extensive min-

occurrence	localities	lithology	grain size	mineralogic composition	dimensions
fluvial terraces	8	sandstone (x-bedded) conglomerate, breccia	0.3 – 5 mm 1 – 50 cm	goethite, hematite, quartz (partly autigenic), pyrite, graphite	100's of metres long, 1 – 5 m thick
bedding-parallel intercalations	4	conglomerate, breccia sandstone	1 – 30 cm 0.1 – 0.3 mm	goethite, hematite, quartz (partly autigenic), pyrite, alunite	up to 200 m long, 0.2 – 2 m thick
ferricrete dykes	12	caliche, breccia, limonite and carbonate clasts	0.3 – 2 mm	goethite, hematite, calcite, dolomite, siderite, apatite manganomelane, gypsum quartz (partly autigenic), markasite, leucophosphite	10's of metres long, 1 – 50 cm thick depth unknown
calcrete dykes	4	caliche, breccia	0.3 – 2 mm	goethite, hematite, calcite, dolomite, pyrolusite, leucophosphite, manganomelane	10's of metres long, 1 – 50 cm thick, depth unknown
sandstone dykes	3	well- to medium-sorted sandstone, composed of quartz and rare claystone	0.2 – 5.0 mm	goethite, hematite quartz, gypsum pyrrhotine, graphite	10's of metres 1 – 50 cm thick depth unknown
breccia dyke	1	poorly to well-sorted breccia	1 – 5 mm	goethite, hematite, gypsum, pyrite, quartz	10's of metres long, 1 – 50 cm thick, depth unknown
claystone dyke	1	bituminous clay	0.05 mm	pyrite, quartz, gypsum, anhydrite, coquimbite, szomolnokite, halite	5 – 10 cm thick, depth unknown
faults & cracks	10	conglomerate, breccia	1 – 10 cm	goethite, hematite, quartz, pyrite	10's of metres long, depth unknown

Table 1. Main properties of mineralized lithologies

eralization, the terraces generally form prominent escarpments (Pl. 1, Fig. 1).

The composition of the terraces is very heterogeneous. Cobbles and pebbles are well-rounded, but very poorly sorted and range from a few cm to several decimetres in size. They are intermingled with clasts of similar size, indicating different distances from the source rock (Pl. 1, Fig. 2). Most common are Cambrian and Ordovician quartzitic sandstones, occasionally with *Tigillites* (*Scolites*) traces, followed by Devonian sandstones and shale fragments of unknown provenance. The finer fraction is composed of hematite-rimmed quartz grains and shale fragments (Pl. 3, Fig. 1). The alterated shale clasts in this sample exhibit small pseudomorphs of hematite after pyrite cubes (Pl. 3, Fig. 2), and tiny flakes of graphite, indicating an originally organic- and pyrite-rich shale. In the laminated crusts surrounding and cementing the clasts, up to 12 alternating bands of goethite and hematite have been counted (sample similar to Pl. 3, Fig. 5).

Bedding-parallel intercalations

These are the most puzzling occurrences of mineralized conglomerates and sandstones because they pretend a much older age than real (WENDT & *al*. 2006, p. 290). They consist of clastics similar to (1) and appear as normally intercalated in the monotonous sequence of grey Upper Devonian shales and sandstones, but wedge out laterally after 100-200 metres. The absence of vertebrate remains, common in similar, but unmistakably Upper Devonian conglomerates, the unusual lithology and the high porosity clearly distinguish these "beds" from the much older host rock. Thus, these lenses are nothing else but erosional furrows, washed out by the early or middle Pleistocene erosion and filled with fluvial gravel, sand and shale which were subsequently mineralized. Most of the shale fragments were altered to a fine-grained, red-coloured mixture of alunite ($KAl_3(SO_4)_2(OH)_6$) and hematite (Pl. 3, Fig. 5). Alunite is not a very common mineral in weathered sedimentary rocks. HOUGH & *al*. (2004) reported its occurrence in the upper part of regolith profiles in the Mount Gibson mine in West Australia. Here, the sulphate appears as a late-stage, pervasive precipitate surrounding clay clasts due to acid sulphate-bearing groundwater solutions. The formation of alunite can be explained by mixing of acid sulphate solutions containing dissolved Al (alteration fluids from shales) with waters of higher pH (groundwater in sandstones?).

Intergranular voids between these components are rimmed with alternating bands of hematite and goethite (Pl. 3, Figs 3, 5). Prior to the oxidation process, the formation of authigenic quartz crystals with pyrite inclusions (Pl. 3, Fig. 4) indicates short periods of mineralization under reducing conditions. This mineral association resembles that of the fluvial terraces (1).

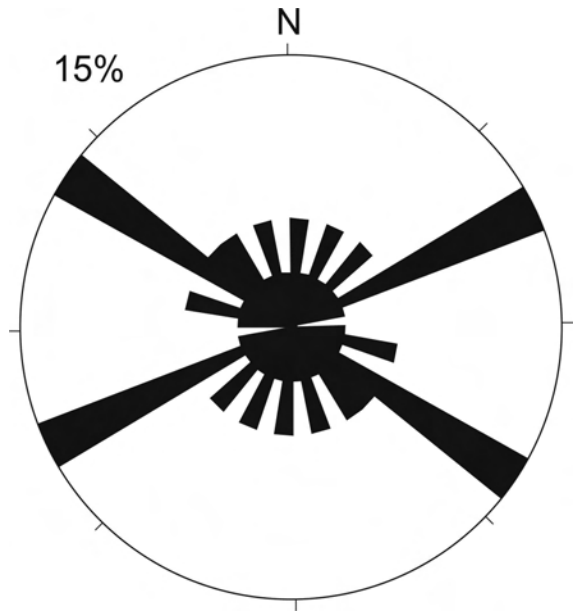

Fig. 3. Rose diagram of the orientation of 64 dykes crosscutting lower Givetian mud buildups. Note predominance of 60°/240° and 120°/300° directions accounting for 60% of measurements

.

Sedimentary dykes

Dark brown to black dykes, a few cm to 0.5 m wide, crosscut many Middle Devonian carbonates (Pl. 1, Fig. 3). Surprisingly, they have been observed only in the Givetian mud buildups (WENDT & *al*. 1997) and their thin onlapping calcareous strata, but never in the surrounding (originally also embedding) argillaceous beds of Late Devonian (Frasnian) age. This fact may be explained by the rather recent exhumation of the mud buildups during the Pleistocene, suggesting a very young age of the infillings. At a first glance, the orientation of the dykes appears random, but a statistical evaluation of 64 measurements shows a predominance of the 60°/240° and the 120°/300° orientations which account for 60% of the obtained data (Text-fig. 3). The dykes were opened by tensional stress perpendicular to the two prevailing directions which may be related to the uplift of the Hoggar Massif (GIROD 1971).

The infilling of the dykes is very heterogeneous and comprises the following lithologies:

Ferricretes

This lithology is most common and was found in the majority of the dykes. Ferricretes fill fine cracks and veins, a few cm wide, which often follow predominant directions (see above) and occasionally also encrust exposed surfaces. Goethite occurs as clasts, spherulitic aggregates (Pl. 4, Fig. 4) and as rims cementing the clasts. A sample from Jebel Tamamat shows peculiar carbonate-hematite intergrowths (Pl. 5, Fig. 3) with a "labyrinthic" internal structure which seam internal cavities. Additional minerals are goethite (Pl. 5, Fig. 4), manganomelane, pyrite and authigenic quartz. Similarly, samples 188/3 and 199/6e are characterized by younger goethite and carbonate mineralizations, embedding older clasts of ferruginous shales and carbonate (Pl. 5, Figs 1-2).

A ferruginous dyke of this type crosscuts a mud mound south of Akabli (loc. 103) and is silicified (silcrete). The primary mineralization consists of large crystals of zoned pyrite and twinned marcasite. Beside tiny relics of pyrite and marcasite in authigenic euhedral quartz crystals (Pl. 4, Fig. 4), the iron sulphides are completely replaced by goethite showing perfect pseudomorphs, in which even the zoning and twinning of the former pyrite and marcasite crystals, respectively, are preserved (Pl. 4, Figs 5, 6). In contrast to other ferricretes, the one of locality 282 is yellow to light brown. Microscopic investigation shows a groundmass of tiny, platy to diamond-shaped crystals (Pl. 5, Fig. 5) with numerous small inclusions of hematite and goethite. This mineral was identified by XRD-analysis as leucophosphite ($KFe_2^{3+}(PO_4)_2OH \cdot 2H_2O$), which is normally found in pegmatites, but occurs also in association with apatite nodules in black shales. Veinlets in the leucophosphite matrix consist of younger collomorph apatite.

The enrichment of secondary phosphates may be derived from phosphate-bearing solutions, which were produced during the alteration of the underlying carbonate rocks or black shales. In the terminology of BEAUVAIS & ROQUIN (1996) all ferricretes belong to the massive type showing colloform and micro-oolitic microstructures.

Calcretes

The depositional history of calcretes is complex and exhibits several phases of reworking and cementation. Clasts are limonitic and calcareous often exhibiting an *in-situ*-fragmentation. The matrix consists of several generations of calcite, dolomite, goethite and quartz which sometimes penetrate or dissect each other (Pl. 3, Fig. 6; Pl. 4, Fig. 1). Various Mn-oxides are the main constituent in a calcrete dyke at Gouiret es Sud (Pl. 4, Fig. 3). A dyke penetrating a mud mound at Gouiret bou el Mout (loc. 83) contains phosphatic, simple and multiple ooids, 0.1 to 0.3 mm in diameter, composed of numerous concentric layers and concentrated in irregular void fillings (Pl. 4, Fig. 2). This mineral, which is also found as slightly larger crystals in the groundmass of the rock, was again identified as leucophosphite. Open pore spaces constitute up to about 10% of the total rock volume.

Sandstones

They consist of small (0.2-1.0 mm), well- to medium-rounded and -sorted or subangular quartz grains which partly show corroded surfaces. In addition, rare elongated (up to 5 mm long) shale clasts and very fine-grained (0.01-0.05 mm) sandstones occur. The components are not or only slightly compacted and rimmed by goethite and hematite leaving many open pore spaces (Pl. 5, Fig. 6). Patchy relics of dissolved idiomorphic gypsum crystals can be distinguished which are partially filled with cloudy hematite (Pl. 6, Fig. 1). In some of the laminated shale clasts, graphite flakes and pseudomorphs after tiny cubes of pyrite can be observed indicating a primary pyrite- and organic-rich mudstone. Alteration of these clasts may result in the formation and the enrichment of secondary gypsum crystals.

Breccias

They consist of dark-brown clasts of limonite and shale, some of the latter containing undeterminable, hematized organic remains (probably ostracods) and tiny pyrite pseudomorphs. Similar to the sandstones, the matrix is formed by laminated goethite/hematite which also fills cracks in the shale clasts. The up to 1 cm long, rounded or angular, claystone fragments are partly replaced by fine-grained iron oxides and hydroxides (Pl. 6, Fig. 2). Some of the small open pore spaces (< 0.2 mm) in the matrix are dissolved gypsum crystals which are internally lined with goethite rims. Large open pore spaces account for about 20% of the total rock volume.

Claystone

The base of the prominent mud mound at the northern margin of Sebkha Mekkerhane (loc. 106; WENDT & KAUFMANN 1998, fig. 5) is dissected by a several cm wide dyke which is filled with dark grey,

organic-rich mudstone. Accurate search for microfossils under the SEM was negative.

The fine-grained iron-rich rock contains numerous pyrite framboids (Pl. 6, Fig. 3), which are probably of bacterial, syn-depositional origin, in a groundmass of globular aggregates of fine-grained quartz and szomolnokite (Pl. 6, Fig. 4), an iron monohydrosulphate ($FeSO_4 \cdot H_2O$). Szomolnokite is a rare mineral, typically formed in pyrite-rich oxidized sulphide deposits under highly acid and arid conditions. Hydrated iron sulphates are also found in coals due to the reaction of pyrite (fine-, rather than coarse-grained) with water percolating in coal seams and associated strata (WIESE & *al*. 1987), and in sandstones intercalated in pyritic coals and black shales (CODY & BIGGS 1973). In the Mount Lofty area in South Australia, SKWARNECKI *et al*. (2002, cited in GEE & ANNAND 2004) reported the presence of secondary framboidal pyrite in a regolith. These pyrites were formed by cyanobacteria in soils of high organic carbon. This bacterial activity reduced soluble sulphate in groundwater rising from underlying sulphide-rich basement rocks.

Younger mineralizations with anhydrite and coquimbite occur along small yellow veinleits of the rock (Pl. 6, Fig. 5). The formation of the trivalent hydrated iron sulphate coquimbite ($Fe_3+2(SO_4)_3 \cdot 9H_2O$) may be the result of sporadic, short introduction of rain water or groundwater along fractures, with subsequent local hydration and oxidation of the szomolnokite-rich clay. In addition, scattered, minute (0.01-0.03 mm) gypsum needles and finely dispersed halite were observed under the SEM. This lithology is rather enigmatic and may be interpreted as a redeposited lacustrine clay derived from one of the lakes which were common in the surroundings during the early Pleistocene (G. CONRAD 1970, fig. 148). The halite is probably of more recent origin, deposited by *in-situ* evaporation or wind-blown from the adjacent sebkha.

Faults and cracks

In two localities on the western margin of the Foum Belrem Ridge (loc. 323 and 370 on Text-fig. 2), lateral and vertical offsets with displacements of a few metres were observed on wind-blown, perfectly exposed surfaces of Famennian shales (Pl. 2, Fig. 1). The fault fissures are filled with a mineralized, coarse conglomerate similar to that of the terraces. The sandstone components of the conglomerate must be far-transported because they have no counterparts in the host rock. They are probably derived from exposures of Lower Palaeozoic rocks from where they were swept by rivers into the easily erodible depressions of Upper Devonian shales. Fragments of shale (usually with graphite and pseudomorphs after pyrite) are partly or totally replaced by hematite and goethite (Pl. 6, Fig. 6). Similar transcurrent faults may be more common but are difficult to observe, because these shales are mostly covered by younger alluvial deposits.

Another tectonic phenomenon are cracks crisscrossing Silurian and Famennian shales, a few cm wide and some metres long and also filled with mineralized conglomerates (Pl. 2, Fig. 2). In contrast to the faults, the cracks do not show any visible lateral or vertical displacement. The best place to observe this feature are the Famennian shales at the northern termination of the Gour-bou-Kreis anticline (loc. 436).

CHEMICAL COMPOSITION

The elemental composition (expressed in atomic weight%) of selected samples of the lithologies described above is listed in Table 2. From this compilation it becomes evident that O, Ca and Fe are the dominant elements generally accounting for more than 80% of the total composition and showing that Fe_2O_3 (hematite), FeOOH (goethite) and $CaCO_3$ (calcite) are the predominant rock forming minerals. Only in one sample (A 161/3a) is Mn present with 37% showing that pyrolusite and other Mn-oxides are the prevailing mineral in an iron-poor calcrete. The relatively high Mg-content in two dyke samples indicates a high amount of dolomite. Si is very high in pebble- and sand-sized clastic lithologies and in silicified ferricretes and calcretes. The relatively high percentage (up to 12%, not shown in Tab. 2) and the origin of phosphorus in three dykes, indicating the presence of the mineral leucophosphite, remains somewhat enigmatic, but must be derived from the underlying black shales.

ORIGIN AND MOBILIZATION OF IRON

Three sources for the precipitation of iron can theoretically be envisaged:

(1) From a hydrothermal source related to the Hoggar volcanism which was simultaneously active farther south (GIROD 1971). This mechanism can be excluded, because all occurrences of mineralized lithologies are unequivocally sedimentary and do not contain any exclusively hydrothermally-generated minerals.

(2) Direct precipitation of iron oxides and hy-

droxides in lakes or swamps during moist intervals (bog ores). Deposits of this kind are widespread in the Sahara (e.g. BUSCHE 1998, pp. 99, 114; FELIX-HENNINGSEN 2000), but always of very limited extend. This process cannot be invoked either for the extensive mineralized terraces or for the extremely local dyke fillings which do not show any relationship to adjacent lacustrine deposits (with the exception of the claystone dyke at loc. 106 which, however, contains only traces of iron).

(3) Erosion and mobilisation of iron from underlying sediments exposed at Plio-/Pleistocene land surfaces. As already pointed out by G. CONRAD (1970, p. 50), iron in mineralized fluvial terraces must be derived from the impermeable, bituminous Lower Silurian or Upper Devonian shales which are rich in pyrite. Alteration and oxidation of metal sulphides in soils leads to the formation of (iron) oxides (SCHIPPERS 2004). Thus, the iron oxide and hydroxite concentrations reflect pluvial phases predating the present extremely arid climate, a process which is widespread under tropical conditions (MAIGNIEN 1959, SCHWERTMANN & TAYLOR 1989). Similar mineralized crusts are also common on top of Lower Devonian sandstones which became emergent and were deeply eroded during the Emsian (WENDT & *al.* 2006). But the study of these mineral incrustations is beyond the scope of the present paper.

DIAGENESIS

All samples from the above listed occurrences exhibit a great variety of early diagenetic stages. Almost ubiquitous are goethite/hematite rims encrusting components (quartz grains, breccia clasts, pebbles and cobbles) lining, however, only their surfaces and leaving large open pore spaces. Macroporosity has roughly been estimated between 10 and 20%; microporosity is up to 10%. Other incompletely filled cavities are cemented by blocky calcite, dolomite or quartz. Authigenic minerals are quartz, gypsum, and various phosphates and sulphates.

The alteration of pyrite is a complex process involving hydration, hydrolysis, and oxidation reactions (JAMBOR & *al.* 2000). The overall process is commonly reported by the following reaction:

$$FeS_2 + 15/4O_2 + 14/4\ H_2O \rightarrow Fe(OH)_3 + 2\ H_2SO_4$$

Kinetics and mechanism of this process depend on temperature, pH, Eh, relative humidity and the available surface of the reacting pyrite. The generated sol-

Sample	Stratigraphic occurrence	Lithology	Analyzed spot	Atomic weight %							
				O	Mg	Al	Si	S	Ca	Mn	Fe
A 215	terrace	sandstone	shale fragment	65		4	11				19
			Fe-crust	68		1	3				29
A 322	terrace	conglomerate	Fe-crust	71		1	1	5			20
			Fe-crust	73		1	2	1			24
A 235	bedding-parallel intercalation	breccia	limonitic grain	57		7	11				21
			fibrous Fe	50							50
A 161/3a	dyke	calcrete	carbonate	50	2	2	2		37		
			Mn-crust	51	3		2		2	37	2
A 161/3c	dyke	calcrete	carbonate	50					48		2
			carbonate	51	17	1	3		24		3
			Fe-crust	53	8	1	4		9		25
A 103B1	dyke	ferricrete	carbonate	50	15				33		1
			Fe-crust	52			4		1		43
A 160/4a	dyke	ferricrete	Fe-crust	53		1	5		11		30
J 22	dyke	sandstone	Fe-crust	77			1	1			19
A 106	dyke	claystone	pyrite framboid	13			1	59			27
			matrix	50			24	11			15
A 323/25	fault plain	conglomerate	Fe-crust	52			1	1			45

Table 2. Chemical composition of Fe-rich phases; minor elements have been omitted, accounting for total < 100%

uble ferric iron cannot coexist with pyrite for longer periods, because the remaining pyrite reduces Fe_3+(aq) by the overall reaction:

$$FeS_2 + 14\ Fe^{3+} + 8H_2O \rightarrow 15\ Fe^{2+} + 2\ SO_4^{2-} + 16H^+$$

Oxidation processes in fine-grained pyrite-rich shales (as in sample A 106/1) occur in a more acidic environment (by production of more sulphuric acid). The initially formed ferric iron will be rapidly transformed back to ferrous iron due to the large surface area of the numerous tiny pyrite crystals (framboids). This produces divalent hydrated iron sulphates, like szomolnokite, which is the main constituent in this sample.

Continuing alteration and/or introduction of external fluids can be observed along small fractures of the rock. At a first step Fe^{2+}-sulphates were oxidized to trivalent hydrated sulphates, like coquimbite (Fe^{3+}+ $2(SO_4)_3 \cdot 9H_2O$), and finally to goethite and gypsum or anhydrite.

In contrast, low quantities of sulphides or large crystals in contact with water keep the fluid near-neutral in pH without the acid production of pyrite oxidation. Large crystals of pyrite (and marcasite), as in sample A 103E2, were converted directly to goethite without the formation of divalent iron minerals. The relatively low surface area of these large sulphides in combination with sufficient pH-buffering capacity of the rock slows the rate of the reduction process, resulting in the formation of pseudomorphs of goethite after pyrite and marcasite.

On the other hand, the presence of Ca- and Fe-sulphates, halite, and gypsum beside pyrite may indicate a more recent acidic saline, sulphate-rich lake environment. Such conditions and mineralizations were reported from saline groundwater discharge lakes, like Lake Tyrell, Victoria, Australia (WELCH & *al*. 2004). Finely interbedded sulphide layers, grey clays and salts (halite and gypsum) in mounded salt crusts, occurring at a distance of a few metres from the shoreline of the lake, are evidence of episodic deposition and biological activity. The formation of the ironsulphides is believed to occur *in situ* as a product of microbiological activity from heterotrophic sulphate reducers.

It has long been known, that significant amounts of sulphides can form in saline inland environments (FITZPATRICK & *al*. 1996). The occurrence of monosulfides and pyrite framboids was reported from superficial, more saline sediments of the Lower Murray floodplains in the Loveday Basin, South Australia (WALLACE & *al*. 2005). The sulphur- bearing mineralization, which is heterogeneously distributed in the upper 0.4 m of the sediment, consists of iron sulphides (pyrite framboids surrounding plant roots), monosulphides and sulphates (jarosite and gypsum).

AGE

We have not been able to date biostratigraphically any of the mineralized lithologies. But several analogies to and close relationships with equivalent deposits described by G. CONRAD (1970) from the same area allow rather reliable datings. This author (1970, p. 215-224) has attributed the upper, heavily mineralized terrace in the Ahnet-Mouydir to the Villafranchian (lowermost Pleistocene), and the middle, equally mineralized terrace in the same area to the middle Pleistocene (1970, p. 241). The latter attribution is based on early Palaeolithic artefacts embedded among the terrace boulders. Artefacts of a similar age (1.6-1.8 Ma) were discovered in the mineralized upper terrace of Jebel Idjerane (Text-fig. 2) by BONNET (1961). Though these discoveries remind one the finding of a needle in a haystack, we cannot cast any doubts on it. We therefore adopt this dating for the upper and middle terrace (which were not individually separated by us in the field) to the lower and middle Pleistocene. The existence of an early Pleistocene pluvial phase in the central Sahara has also been demonstrated by K/Ar-ages of basaltic lavas in the Hoggar Massif (ROGNON & *al*. 1981) which are considered as contemporaneous with the terraces.

As pointed out above, the bedding-parallel, conglomeratic intercalations in Upper Devonian shales and sandstones are characterized by the same lithology, mineral composition and porosity as the terraces, suggesting a similar age. The same assumption is obvious for the conglomerate-filled fault fissures and cracks. The infillings of the majority of the dykes, however, do not show any direct relationship to these fluvial deposits. They were tectonically opened by internal forces and subsequently filled with various, subaerially deposited, mineralized sediments which have preserved high porosities (ferricretes, calcretes, poorly cemented sandstones and breccias). This composition suggests an equally recent origin which we tentatively also attribute to the lower or middle Pleistocene. This supposition is corroborated by the occurrence of gypsum and anhydrite in some of the samples. Both minerals do not occur in any of the underlying or encasing Palaeozoic rocks, but are common on weathered surfaces of Silurian and Devonian shales, as well as in Pleistocene to Recent sebkhas (G. CONRAD 1970, p. 395-413). It is very improbable that gypsum crystals in sandstone dykes (e. g. in loc. 22 and 50) were me-

chanically introduced (and if so, they could only be derived from weathered clays in the vicinity). They must be the result of evaporation under (sub)recent arid conditions. Thus, a Pleistocene age of the dykes is strongly suggested.

DISCUSSION AND CONCLUSIONS

The inferred lower/middle Pleistocene land surface along the northern margin of the Hoggar Massif is sketched on Text-figure 4. The composition and age of the mineralized terraces are the clue for deciphering the role and extent of the tectonic or seismic activities, exemplified by dykes, faults and cracks in the underlying or encasing older rocks. At a frist glance, the occurrence of Pleistocene terraces left behind by a widespread river system under tropical pluvial conditions, and the infilling of opened dykes, cracks and faults appear as two processes which have nothing in common with each other. But their corresponding lithologies reveal a close relationship between the two different depositional environments which we explain by their approximately same age. This interpretation is strongly supported by the identical mineral phases cementing and encrusting the transported and loosely packed components. The high porosity and the presence of large open pore spaces in both, terraces and infillings of tectonically induced cavities, as well as the only slight or lacking deformation of clay/shale clasts between quartz grains (Pl. 3, Figs 1, 2; Pl. 5, Fig. 6) indicate the absence of noticeable diagenetic processes and a very young age of the cavity fillings.

Sedimentary dykes must not necessarily have a tectonic origin. A great number of dyke-forming processes (desiccation, syneresis, gravitational sliding, subsidence, karstification, temperature difference, tectonic stress and others) have been discussed in the past (STRAUCH 1966, DEMOULIN 2003). Recent contributions to this topic (MONTENAT & *al*. 2007) distinguish between intrusion dykes (filled from below) and neptunian dykes (filled from above), irrespective of the origin of the infilling sediment. However, we prefer the general term sedimentary dykes for the latter, because "neptunian" reminds one of Neptune, the mythological god of the sea, thus suggesting an exclusively marine infilling.

In the examples described in the present article, factors other than tectonic or seismic activity can be excluded as responsible for the formation of the dykes. This origin is documented by the corresponding walls and the preferred, often parallel directions of the dykes (Text-fig. 3). Unfortunately their depth of penetration remains unknown, because all observations were made on weathered surfaces, and levels deeper than a few metres are not exposed.

Two major types of dyke fillings can be distinguished: (1) poorly sorted breccias and well-sorted quartz sandstones, and (2) ferricretes, calcretes and silcretes. Type (1) is clearly of fluvial origin reflecting transport by rivers and is related to similar deposits of terraces in the vicinity. In contrast, type (2) is an *in-situ* deposit. Calcretes are formed by ascending waters in combination with capillary rise, evaporation and mixing of vadose and phreatic waters in semiarid environments (WRIGHT & TUCKER 1991). Ferricretes form under tropical, humid or alternating humid to dry conditions (BATTIAU-QUENY 1996, BEAUVAIS & ROQUIN 1996 and others) and can be deposited extremely rapidly (PHILLIPS 2000). Such a climate existed during the early and middle Pleistocene in the Hoggar area (G. CONRAD 1970, p. 224, 439, 457). Silcretes are of pedogenic or groundwater origin. In addition, one claystone dyke has been observed which displays very complex diagenetic alterations of a presumed lacustrine deposit.

This first direct evidence of neotectonic phenomena confirms the hitherto rather vague ideas about young intracratonic deformation along the northern border of the Hoggar Massif. The great variety of lithologies related to these tectonic phenomena reflect

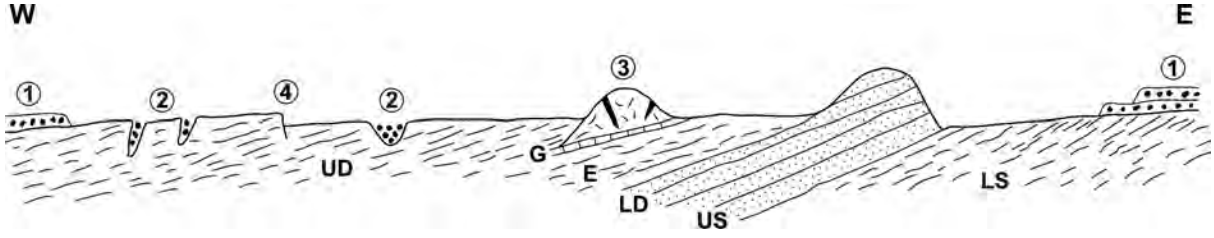

Fig. 4. Idealized sketch of the inferred lower/middle Pleistocene land surface along the northern margin of the Hoggar Massif (not to scale, dip of strata exaggerated). 1 – fluvial terraces, 2 – bedding-parallel erosional furrows, 3 – mud mound with tectonic dykes, 4 – fault. UD – Upper Devonian, G – Givetian, E – Eifelian, LD – Lower Devonian, US – Upper Silurian, LS – Lower Silurian

oscillating climatic conditions in an early phase of desertification of the Algerian Sahara. The accumulation of fluvial terraces and the formation of concomitant erosional furrows as well as some sandstone infillings of dykes represent pluvial phases. Ferricretes and calcretes were deposited during intermittent, more arid intervals of the early and middle Pleistocene.

Acknowledgements

The present contribution is the result of numerous, first accidental, then target-oriented observations and the examination of samples collected during nine expeditions (1992-2006) into the Algerian Sahara with the principal topic of a biostratigraphic and sedimentologic study of the Devonian. The aid of B. KAUFMANN (Graz, Austria) and many students in the field is gratefully acknowledged. Technical assistance was provided by W. GERBER, I. GILL-KOPP, P. JEISECKE (all Tübingen) and B. KAUFMANN (Graz, Austria). We also want to thank C. BERTHOLD (Tübingen) for the performance of XRD. The elaboration of the results benefitted from discussions with F. ALAILY (TU Berlin), D. BUSCHE (Würzburg), J. KUHLEMANN, G. MARKL and J. NEUGEBAUER (all Tübingen), as well as the review by Z. BELKA (Poznan, Poland) and an anonymous reviewer. Field work was funded by the Deutsche Forschungsgemeinschaft (grants We 239.15/1-4).

REFERENCES

BATTIAU-QUENY, Y. 1996. A tentative classification of paleoweathering formations based on geomorphological criteria. *Geomorphology*, **16**, 87-102.

BAUMHAUER, R., BUSCHE, D. & SPONHOLZ, B. 1989. Reliefgeschichte und Paläoklima des saharischen Ost-Niger. *Geographische Rundschau*, **41**, 493-499.

BEAUVAIS, A. & ROQUIN, C. 1996. Petrological differentiation patterns and geomorphic distribution of ferricretes in Central Africa. *Geoderma*, **73,** 63-82.

BERTRAND, J.-M., CABY, R. & LEBLANC, M. 1983. La zone mobile pan-africaine de l'Afrique de l'Ouest. *In*: J. FABRE (*Ed*.), Lexique Stratigraphique International, Nouvelle série, **1**. Afrique de l'Ouest. Introduction géologique et termes stratigraphiques, pp. 35-42. *Pergamon Press*; Oxford – New York – Toronto – Sidney – Paris – Frankfurt.

BEUF, S., BIJU-DUVAL, B., DE CHARPAL, O. ROGNON, P., GARIEL, O. & BENNACEF, A. 1971. Les grès du Paléozoïque inférieur au Sahara. Sédimentation et discontinuités, évolution structurale d'un craton. *Publications de l'Institut Français du Pétrole, Collection "Science et Technique du Pétrole*", N. **18**, pp. I-XV, 1-464. *Éditions Technip*; Paris.

BIROT, P., CAPOT-REY, R. & DRESCH, J. 1955. Recherches morphologiques dans le Sahara central. *Travaux de l'Institut de Recherches Sahariens*, **13**, 13-75.

BIROT, P. & DRESCH. J. 1955. Une faille du Quaternaire récent dans la plaine d'Amguid (Hoggar septentrional). *Societé Géologique de France, Compte Rendu Sommaire des Séances*, **1955**, 209-211.

BONNET, A. 1961. La "Pebble culture" in situ de l'Idjerane et les terrasses de piedmont du Sahara central. *Bulletin de la Societé Préhistorique Française*, **58**, 51-61.

BUSCHE, D. 1998. Die zentrale Sahara. Oberflächenformen im Wandel, pp. 1-284. *Justus Perthes*; Gotha.

CHOROWICZ, J. & FABRE, J. 1997. Organization of drainage networks from space imagery in the Tanezrouft plateau (Western Sahara): implications for recent intracratonic deformations. *Geomorphology*, **21**, 139-151.

CODY, R. D. & BIGGS, D. L. 1973. Halotrichite, szomolnokite, and rozenite from Dolliver State Park, Iowa. *Canadian Mineralogist*, **11**, 958-970.

CONRAD, G. 1970. L'évolution continentale post-hercynienne du Sahara Algérien (Saoura, Erg Chech-Tanezrouft, Ahnet-Mouydir). *Centre de Recherches sur les Zones Arides, Série: Géologie*, **10**, 1-527. *Éditions du Centre National de la Recherche Scientifique*; Paris.

CONRAD, G. & CONRAD, J. 1982. La zone de jonction des cratons de l'Ouest africain et du Sahara central au Cénozoïque: évolution sédimentaire et structurale de l'Ahnet et des confins Erg Chech-Tanezrouft. *In*: LANG, J. (*Ed.*), Livre Jubilaire Gabriel Lucas. Géologie sédimentaire. *Mémoires Géologiques de l'Université de Dijon*, **7**, 391-400.

CONRAD, J. 1972. Distension jurassique et tectonique éocrétacée sur le Nord-Ouest de la plate-forme africaine (Bassin de Reggan, Sahara central). *Comptes Rendus hebdomadaires des Séances de l'Académie des Sciences, Série II*, **274**, 2423-2426.

— 1981. La part des déformations posthercyniennes et de la néotectonique dans la structuration du Sahara central, un domaine relativement mobile de la plate-forme africaine. *Comptes Rendus des Séances de l'Académie des Sciences, Série II: Mécanique, Physique, Chimie, Sciences de l'Univers, Sciences de la Terre*, **292**, 1053-1056.

— 1984. Les séries carbonifères du Sahara central algérien. Stratigraphie, sédimentation, évolution structurale. *Thèse de Doctorat d'Etat ès-Sciences Naturelles. Université Aix-Marseille*, pp. 1-370.

DEMOULIN, A. 2003. Clastic (neptunian) dykes and sills. *In*: MIDDLETON, G.V., CHURCH, M J., CONIGLIO, M., HARDIE, L.A. & LONGSTAFFE, F.J. (*Eds*), Encylopedia of sedi-

ments and sedimentary rocks, 136-137. *Kluwer Academic Publishers*; Dordrech – Boston – London.

FABRE, J. 1976. Introduction à la géologie du Sahara algérien et des régions voisines. I. La couverture phanérozoique. Avec la collaboration de R. CABY, M. GIROD, A. MOUSSINE-POUCHKINE, pp. 1-421. *Societé Nationale d'Édition et de Diffusion*; Alger.

FELIX-HENNINGSEN, F. 2000. Paleosols on pleistocene dunes as indicators of paleo-monsoon events in the Sahara of East Niger. *Catena*, **41**, 43-60.

FITZPATRICK, R W., FRITSCH, E. & SELF, P.G. 1996. Interpretation of soil features produced by ancient and modern processes in degraded landscapes. V. Development of saline sulfidic features in non-tidal seepage areas. *Geoderma*, **69**, 1-29.

FOLLOT, J. 1952. Ahnet et Mouydir. *XIX^{me} Congrès Géologique International, Monographies Régionales, 1re Série: Algérie*, **1**, 1-80, Alger.

— 1953**.** Sur les différentes phases tectoniques ayant affecté la bordure septentrionale du Hoggar. *Travaux de l'Institut de Recherches Sahariennes*, **9**, 137-142.

GEE, R.D. & ANAND, R.R. 2004. Advances in regolith research. A CRC LEME (Cooperative Research Centre for Landscape Environments and Mineral Exploration) Perspective. *Conference Proceedings*, 29-44. PACRIM; Adelaide, SA.

GIROD, M. 1971. Le massif volcanique de l'Atakor (Hoggar, Sahara Algérien). Étude pétrographique, structurale et volcanologique. *Publications du Centre de Recherches sur les Zones Arides, Série Géologie,* **12**, 1-158.

GUIRAUD, R., BELLION, Y., BENKHELIL, J. & MOREAU, C. 1987. Post-Hercynian tectonics in northern and western Africa. *Geological Journal*, **22**, Winter Thematic Issue, African Geology Reviews, 433-466.

HANCOCK, P. L. (*Ed.*) 1994. Continental deformation, pp. I-VIII, 1-421. *Pergamon Press*; Oxford – New York – Seoul – Tokyo.

HOUGH, R., PHANG, C., NORMAN, M. & ANAND, R. 2004. Alunite as a mineral host in ferricrete from the Enterprise pit, Mount Gibson gold deposit. *In*: ROACH, I.C. (*Ed.*) Regolith 2004, Cooperative Research Centre for Landscape Environments and Mineral Exploration (CRC LEME), 144-145.

JAMBOR, J.L., NORDSTROM, D.K. & ALPERS, C.N. 2000. Metal-sulfate salts from sulfide mineral oxidation. *In*: ALPERS, C.N., JAMBOR, J.L. & NORDSTROM, D.K. (*Eds*), Sulfate minerals. *Reviews in Mineralogy & Geochemistry*, *Mineralogical Society of America*, **40**, 303-350.

LARRASOANA, J.C., ROBERTS, A.P., ROHLING, E.J., WINKLHOFER, M. & WEHAUSEN, R 2003. Three million years of monsoon variability over the northern Sahara. *Climate Dynamics*, **21**, 689-698.

LÜNING, S., CRAIG, J., LOYDELL, D.K., STORCH, P. & FITCHES, B. 2000. Lower Silurian 'hot shales' in North Africa and Arabia: regional distribution and depositional model. *Earth-Science Reviews*, **49**, 121-200.

MAIGNIEN, R. 1959. Le cuirassement des sols en Guinée, Afrique occidentale. *Mémoires du Service de la Carte Géologique d'Alsace et Lorraine*, **16**, 3-239.

MONOD, T. 1964. The late Tertiary and Pleistocene in the Sahara and adjacent southerly regions. *In*: F.C. HOWELL & F. BOURLIÈRE (*Eds*), African ecology and human evolution. *Viking Fund Publications in Anthropology*, **36**, 117-229. *Methuen & Co. Ltd*; London.

MONTENAT, C., BARRIER, P., OTT D'ESTEVOU, P. & HIBSCH, C. 2007. Seismites: An attempt at critical analysis and classification. *Sedimentary Geology*, **196**, 5-30.

PHILLIPS, J. 2000. Rapid development of ferricretes on a subtropical valley side slope. *Geografiska Annaler, Series A, Physical Geography*, **82A**, 69-78.

ROGNON, P. 1967a. Le Massif de l'Atakor et ses bordures (Sahara central). Étude géomorphologique. *Centre de Recherches sur les Zones Arides. Série: Géologie*, **9**, 1-559.

— 1967b. Climatic influences on the African Hoggar during the Quaternary based on geomorphologic observations. *Annals of the Association of American Geographers*, **57**,115-127.

— 1989. Biographie d'un desert, pp. 1-347. *Plon*; Paris.

ROGNON, P., GOURINARD, Y. & BANDET, Y. 1981. Un épisode de climat aride dans l'Atakor (Hoggar) vers 1,5 Ma (datations K/Ar) et sa place dans le contexte paléoclimatique du Plio-Pléistocène africain. *Bulletin de la Societé Geologique de France*, (7) **23**, 313-318.

SCHIPPERS, A. 2004. Biogeochemistry of metal sulfide oxidation in mining environments, sediments, and soils. *Geological Society of America, Special Paper,* **379**, 49-62.

SCHWERTMANN, U. & TAYLOR, R.M. 1989. Iron oxides. *In*: B. DIXON & S.B. WEED (*Eds*), Minerals in soil environments. Second edition, Madison, Wisconsin (Soil Science Society of America), 379-438.

SKWARNECKI, M. S., FITZPATRICK, R.W. & DAVIES, P.J. 2002. Geochemical dispersion at the Mount Torrens Pb-Zn prospect, South Australia, with particular emphasis on acid sulphate soils. *Cooperative Research Centre for Landscape Environments and Mineral Exploration (CRC LEME) Restricted Report*, **174**, 1-68.

SMITH, B., DERDER, M.E.M., HENRY, B., BAYOU, B., YELLES, A.K., DJELLIT, H., AMENNA, M., GARCES, M., BEAMUD, E., CALLOT, J.P., ESCHARD, R., CHAMBERS, A., AIFA, T., AIT OUALI, R. & GANDRICHE, H. 2006. Relative importance of the Hercynian and post-Jurassic tectonic phases in the Saharan platform: a paleomagnetic study of Jurassic sills in the Reggane Basin (Algeria). *Geophysical Journal International*, **167**, 380-396.

STRAUCH, F. 1966. Sedimentgänge von Tjörnes (Nord-Island) und ihre geologische Bedeutung. *Neues Jahrbuch für Geologie und Paläontologie, Abhandlungen,* **124**, 259-288.

WALLACE, L., WELCH, S.A., KIRSTE, D., BEAVIS, S. & MCPHAIL, D.C. 2005. Characteristics of inland acid sulfate soils of the lower Murray floodplains, South Australia. *In*: I.C. ROACH (*Ed.*), Regolith 2005 – Ten Years of Cooperative Research Centre for Landscape Environments and Mineral Exploration, 326-328.

WELCH, S. A., BEAVIS, S., & SOMERVILLE, P. (2004). Biogeochemistry at Lake Tyrrell. *In*: I.C. ROACH (*Ed.*), Regolith 2004. Cooperative Research Centre for Landscape Environments and Mineral Exploration (CRC LEME), 391-393.

WENDT, J., BELKA, Z., KAUFMANN, B., KOSTREWA, R. & HAYER, J. 1997. The world's most spectacular carbonate mud mounds (Middle Devonian, Algerian Sahara). *Journal of Sedimentary Research*, **67**, 424-436.

WENDT, J. & KAUFMANN, B. 1998. Mud buildups on a Middle Devonian carbonate ramp (Algerian Sahara). *In*: V.P. WRIGHT & T.P. BURCHETTE (*Eds*), Carbonate Ramps. *Geological Society London, Special Publication*, **149**, 397-415.

WENDT, J., KAUFMANN, B., BELKA, Z., KLUG, C. & LUBESEDER, S. 2006. Sedimentary evolution of a Palaeozoic basin and ridge system: the Middle and Upper Devonian of the Ahnet and Mouydir (Algerian Sahara). *Geological Magazine*, **143**, 269-299.

WIESE, R.G., POWELL, M.A. & FYFE, W.S. 1987. Spontaneous formation of hydrated iron sulfates on laboratory samples of pyrite- and marcasite-bearing coals. *Chemical Geology*, **63**, 29-38.

WRIGHT, V.P. & TUCKER, M.E. 1991. Calcretes: an introduction. *In*: V.P. WRIGHT & M.E. TUCKER (*Eds*), Calcretes. Reprint Series volume 2 of the International Association of Sedimentologists, pp. 1-22. *Blackwell*; Oxford.

Manuscript submitted: 5th September 2007
Revision version accepted: 20th December 2007

Appendix: Coordinates of sample localities in Text-fig. 2
(locality names from Carte Topographique du Sahara 1 : 200 000)

No.	locality, type	coordinates
10	Gouiret es Sud, mud ridge, dyke	N 25° 47,498’; E 1° 16,560’
22	Oued Ouzdaf, mud atoll, dyke	N 26° 34,796’; E 1° 4,880’.
50	Azel Matti, mud mound, dyke	N 25° 35,217’; E 0° 56,430’
67	Gouiret es Sud, mud ridge, dyke	N 25° 47,498’; E 1° 16,560’
68	Gouiret es Sud, mud ridge, dyke	N 25° 49,887’; E 1° 15,936’
83	Gouiret bou el Mout, mud mound, dyke	N 26° 5,777’; E 1° 14,054’
103	S of Akabli, mudmound, dyke	N 26° 35,547’; E 1° 17,718’.
106	N of Sebkha Mekkerhane, mud mound, dyke	N 26° 28,264’; E 1° 11,687’
118	Oued Ouzdaf, mud atoll, dyke	N 26° 34,131’; E 1° 5,002’
160	Gouiret es Sud, mud ridge, dyke	N 25° 52,152’; E 1° 16,226’.
161	Gouiret es Sud, mud ridge, dyke	N 25° 53,460’; E 1° 16,189’.
188	Oued Ouzdaf, mud atoll, dyke	N 26° 34,796’; E 1° 5,795’.
199	S of Jebel Tamamat, mud mound, dyke	N 26° 3,924’; E 0° 44,457’.
200	S of Jebel Tamamat, mud ridge, dyke	N 26° 5,054’; E 0° 43,898’
215	E of Erg Tagsist, terrace	N 25° 12,327’; E 1° 33,159’.
235	W of Erg Teganet, bedding-par. intercalation	N 26° 23,719’; E 4° 3,733’.
282	Gouiret bou el Mout, mud atoll, dyke	N 26° 6,049’; E 1° 15,189’.
285	S of Azel Matti, terrace	N 25° 25,095’; E 0° 54,144’.
308	E of Hassi el Krenig, terrace	N 26° 28,896’; E 3° 8,053’.
310	W of Ain Tahaia, terrace	N 26° 26,751’; E 3° 44,091’.
312	E of Ain Bagline, bedding-par.intercalation	N 26° 16, 671’; E 3° 47,453’.
316	E of Jebel Bagline, terrace	N 26° 08,784’; E 3° 53,917’.
322	E of Ain Behaga, bedding-par. intercalation	N 26° 50,025’; E 3° 41,595’.
323	S of Ain Kahla, fault	N 27° 18,565’; E 3° 28,966’.
370	Jebel Azaz, fault	N 27° 08,902’; E 3°, 25,615’.
377	NE of Kranguet el Hadid, terrace	N 26° 28,359’; E 4° 43,179’.
380	W of Hassi Tahaft, terrace	N 26° 16,389’; E 6° 19,688’.
381	W of Hassi Tahaft, terrace	N 26° 14,342’; E 6° 21,825’.
430	Jebel Mouima, bedding-parallel intercalation	N 25° 53,246’; E 2° 51,340’.
436	Gour bou Kreis, crack	N 26° 27,439’; E 3°9,211’.

PLATES 1-6

PLATE 1

1 – Mineralized upper (in the background) and middle terrace in the Iraouene Mountains along the trail from Hassi Habadra to Amguid (loc. 380).

2 – Irregular contact between bleached and eroded Lower Silurian shales (hammer) and overlying mineralized middle terrace. Same area as Fig. 1).

3 – Two sub-parallel mineralized dykes, crosscutting crinoidal limestone onlapping flank of Givetian mud atoll, Oued Ouzdaf (loc. 22). Coin is 2.5 cm.


1

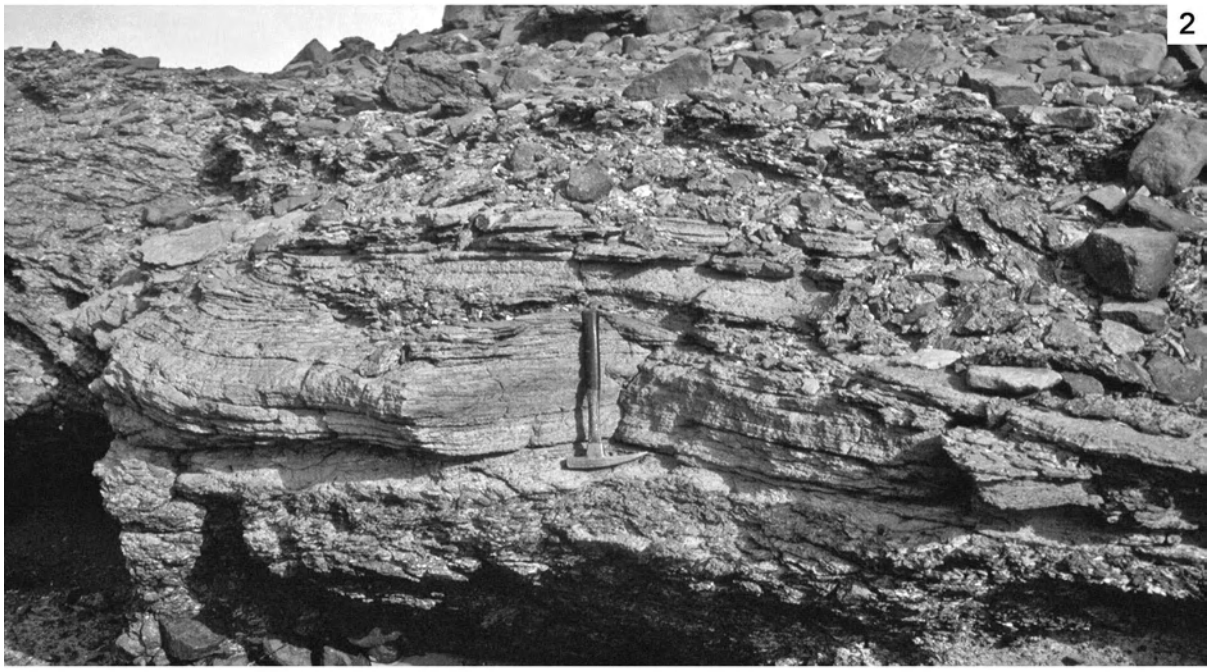
2


3

PLATE 2

1 – Mineralized and conglomerate-filled fault-fissure, displacing Famennian shales. Lateral movement indicated by white arrows. 10 km S of Ain Kahla (loc. 323). Hammer is 35 cm long.

2 – Vertical crack (arrowed) crosscutting upper Famennian shales and filled with mineralized conglomerate. Jebel Azaz (loc. 370). Hammer (*) is 35 cm long.

1

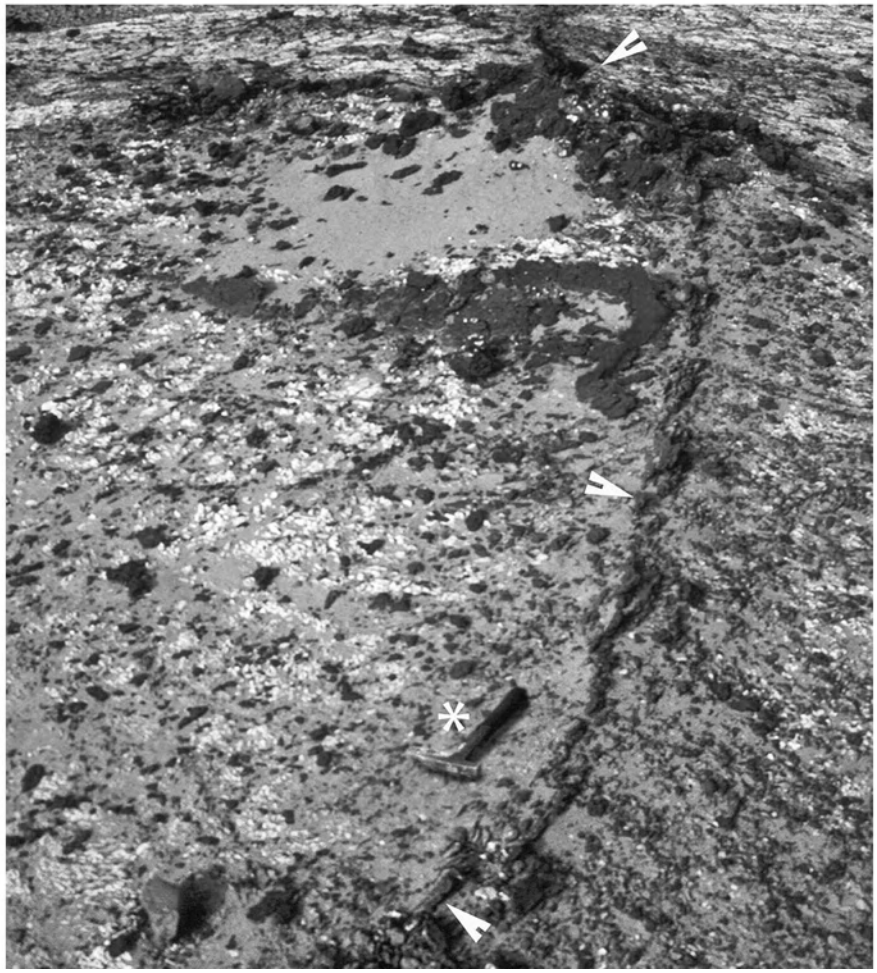

2

PLATE 3

1 – Sandstone intercalated in Pleistocene terrace overlying upper Frasnian sandstones, E of Jebel Bagline (loc. 316). Slightly compacted quartz grains and large flake of shale, rimmed by thin hematite seams (white). Sample 316/3. Photomicrograph 21_02, reflected light, width of field 1.4 mm.

2 – Same sample as Fig. 1. Two fragments of shale with relics of pyrite (hematite pseudomorphs) surrounded by hematite rim (white). Photomicrograph 21_10, reflected light, oil immersion, width of field 0.7 mm.

3 – Bedding-parallel intercalation of conglomeratic sandstone in Famennian shale, E of Ain Behaga (loc. 322). Hematite (white) and goethite (blue) crusts on shale remnants (light brown) with authigenic quartz crystals (dark brown). Sample 322. Photomicrograph 21_22, reflected light, oil immersion, width of field 0.7 mm.

4 – Brecciated bedding-parallel intercalation in upper Frasnian sandstones, W of Erg Teganet (loc. 235). Authigenic quartz crystals (grey) with pyrite inclusions in a hematite/goethite matrix. Sample 235a. Photomicrograph 35_25, reflected light, width of field 1.4 mm.

5 – Same sample as Fig. 4. Collomorph hematite (white)-goethite (blue) crusts around shale clasts consisting of hematite and alunite (al). Photomicrograph 20_01, reflected light, oil immersion, width of field 0.7 mm.

6 – Calcrete dyke in Givetian mudridge, Gouiret es Sud (loc. 160). Corroded limonite clasts in coarsely crystalline carbonate cement (grey). Sample 160/4a. Photomicrograph 29_16, reflected light, width of field 1.4 mm.

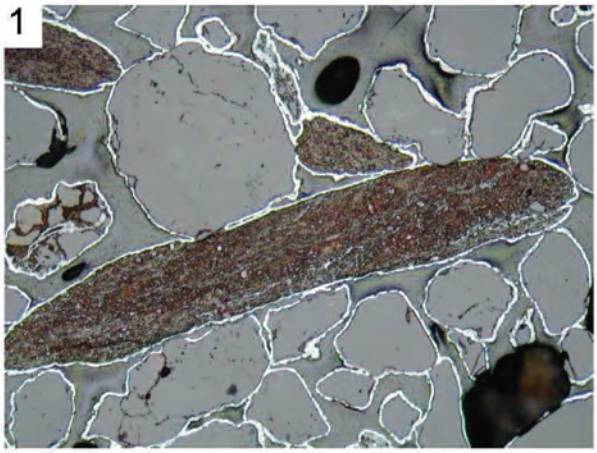
1

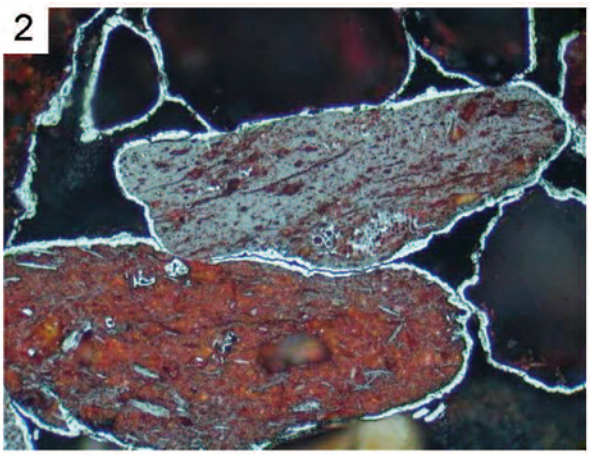
2

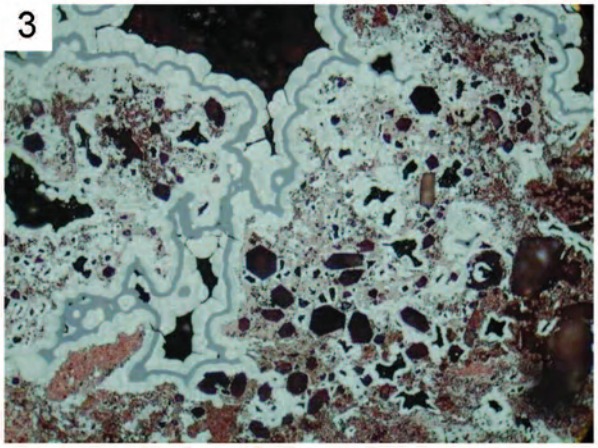
3

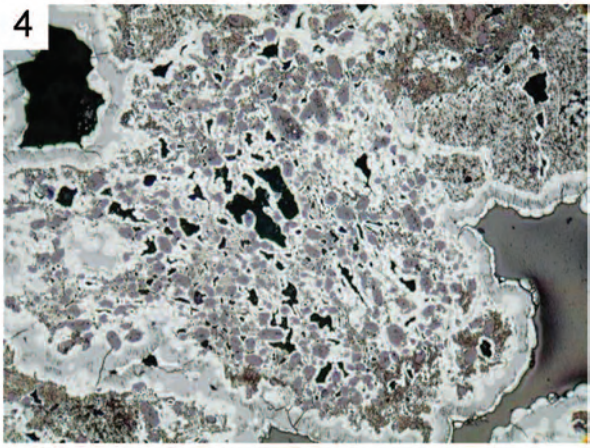
4

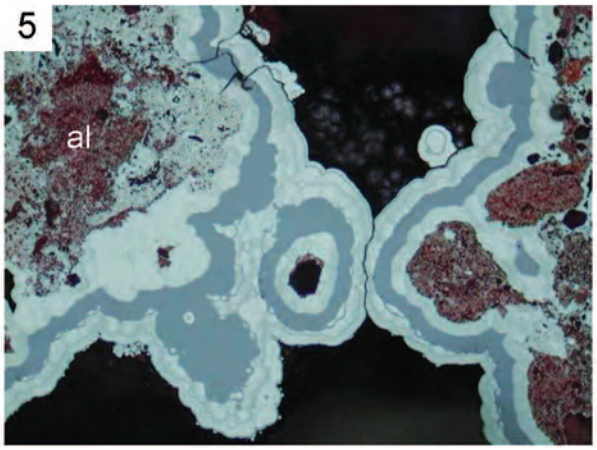
5
al

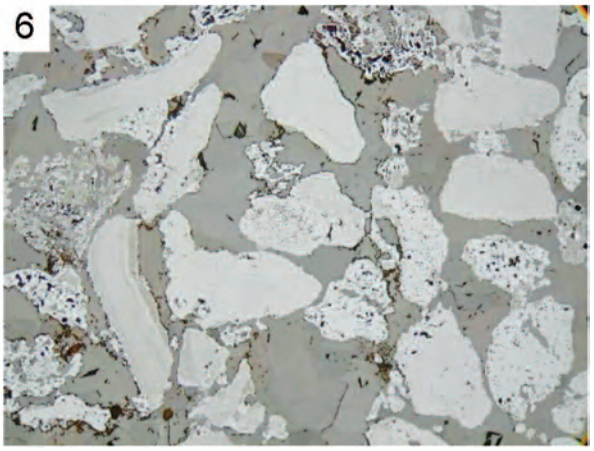
6

PLATE 4

1 – Same sample as Pl. 3, Fig. 6. Corroded carbonate grain (grey), partially replaced by goethite (white) and surrounded by younger blocky calcite cement (dark grey). Photomicrograph 35_26, reflected light, width of field 1.4 mm.

2 – Calcrete dyke in Givetian mud mound, Gouiret bou el Mout (loc. 83). Simple and multiple ooids of leucophosphite in an irregular void filling. Sample 83/8S. Photomicrograph 36_32, transmitted light, crossed polars, width of field 2.8 mm.

3 – Calcrete dyke in Givetian mud ridge, Gouiret es Sud (loc. 161). Mn-oxides (black spots), pyrolusite (grey, right), manganomelane (white, left) and limonite (various shades of grey). Sample 161/3a. Photomicrograph 29_15, reflected light, width of field 1.4 mm.

4 – Silicified ferricrete dyke in Givetian mud mound S of Akabli (loc. 103). Former aggregates of pyrite crystals replaced by fine-grained goethite (olive green, right). Relics of pyrite in newly formed authigenic quartz crystals (arrow), scattered goethite ooids (blue) on left margin. Sample 103E2. Photomicrograph 36_12, reflected light, oil immersion, width of field 0.7 mm.

5 – Same sample as Fig. 4. Pseudomorphism of goethite after pyrite cube (right), surrounded by goethite spherulites (black, left). Photomicrograph 36_15, reflected light, crossed polars, oil immersion, width of field 0.7 mm.

6 – Same sample as Fig. 4. Pseudomorphism of goethite after marcasite twins. Note small authigenic quartz crystals (dark brown) with tiny inclusions of marcasite relics. Photomicrograph 36_17, reflected light, oil immersion, width of field 0.7 mm.

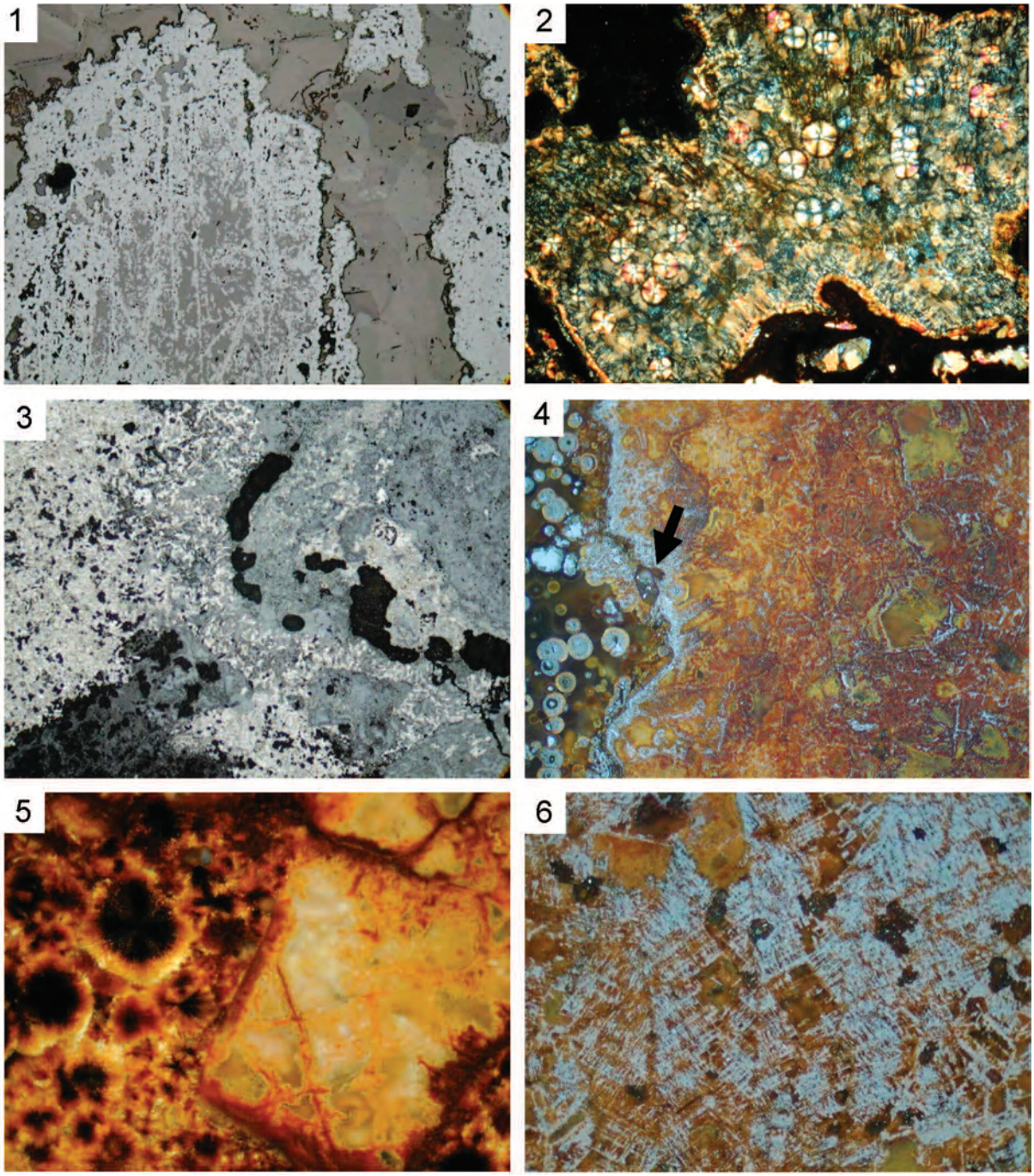
1
2
3
4
5
6

PLATE 5

1 – Ferricrete dyke in Givetian crinoidal limestone, Oued Ouzdaf (loc. 188). Euhedral carbonates (grey) overgrown by goethite crystals (white). Sample 188/3. Photomicrograph 34_15, reflected light, width of field 1.4 mm.

2 – Same sample as Fig. 1. Elongated goethite clast veined by younger coarse grained goethite. Photomicrograph 34_24, reflected light, crossed polars, oil immersion, width of field 0.7 mm.

3 – Ferricrete dyke in Givetian mud ridge, S of Jebel Tamamat (loc. 200). Former open space rimmed by carbonate cushion-shaped, "labyrinthic" carbonate (dark) - hematite (white) intergrowths and occluded by later carbonate (dark brown). Sample 200/2. Photomicrograph 29_21, reflected light, oil immersion, width of field 0.7 mm.

4 – Same sample as Fig. 3. Spherolites of goethite (dark brown) overgrown by fibrous (light brown) and blocky (white) calcite. Photomicrograph 35_21, transmitted light, crossed polars, width of field 2.8 mm.

5 – Ferricrete dyke in Givetian mud atoll, Gouiret bou el Mout (loc. 282).Tabular crystals of leucophosphite (grey) with tiny inclusions of hematite (white, right) and goethite (light grey, left). Note authigenic quartz crystals (dark brown). Sample 282a. Photomicrograph 29_27, reflected light, width of field 1.4 mm.

6 – Sandstone dyke in Givetian mud mound, Azel Matti (loc. 50). Well-rounded quartz grains (grey) and large shale fragment (brown) rimmed by laminated goethite. Sample 50/1a. Photomicrograph 20_07, reflected light, width of field 1.4 mm.

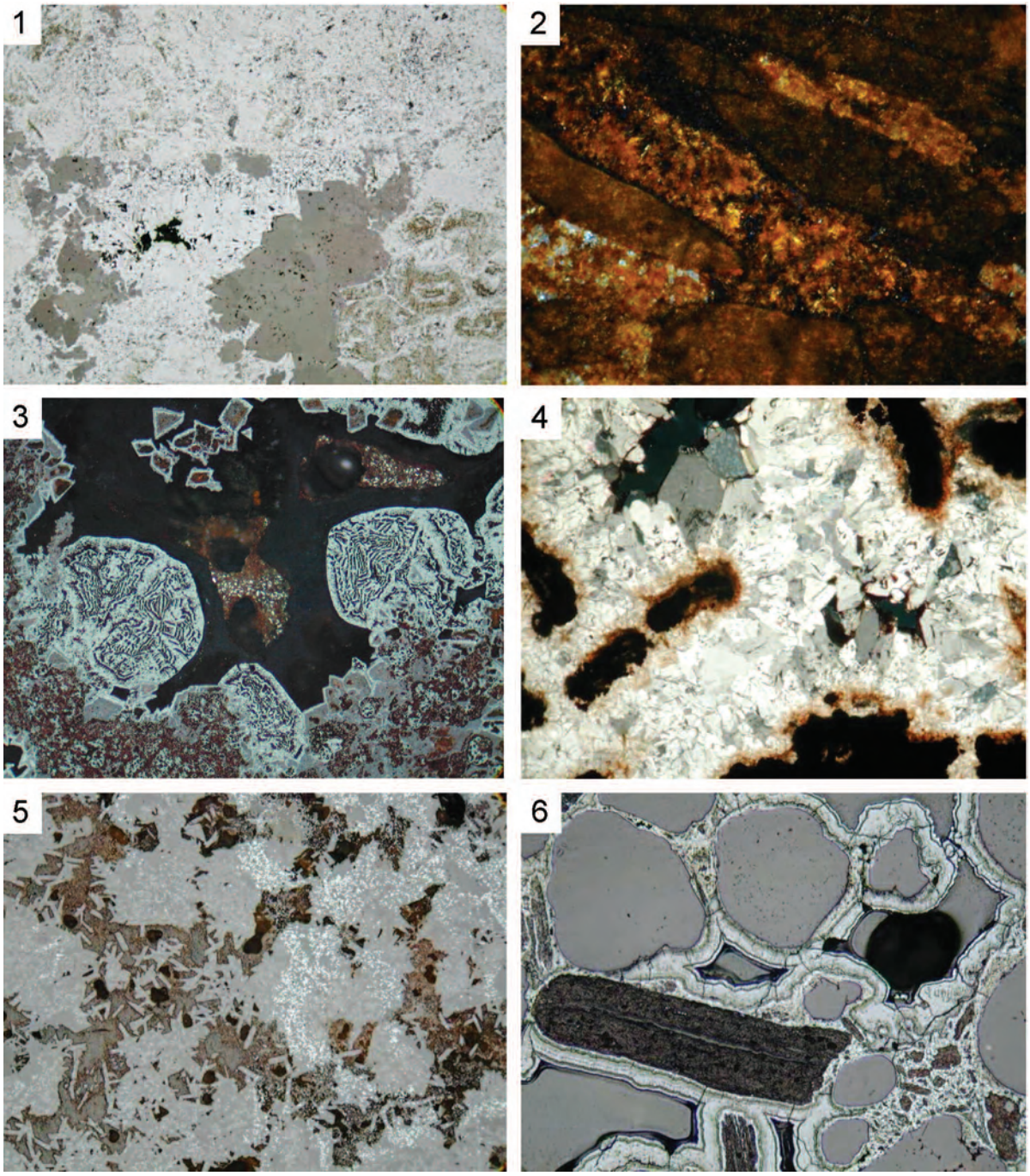
1
2
3
4
5
6

PLATE 6

1 – Same sample as Pl. 5, Fig. 6. Shale fragments (brown) and prismatic aggregates of goethite and hematite. The rims of the prisms consist of goethite, the cores are filled with collomorph hematite (white) indicating secondary open spaces. The tabular shape is interpreted as pseudomorphs after platy gypsum crystals. Photomicrograph 20_09, reflected light, oil immersion, width of field 0.7 mm.

2 – Breccia dyke in Givetian mud mound, Azel Matti (loc. 50). Goethite and hematite aggregates (white) replacing shale clasts (brown) and probable gypsum crystals (light grey). Open voids are rimmed by laminated goethite/hematite. Sample 50/1b. Photomicrograph 35_02, reflected light, width of field 1.4 mm.

3 – Claystone dyke in Givetian mud mound N of Sebkha Mekkerhane (loc. 106). Tiny cubes of pyrite in framboid-type arrangements. Sample 106/1. Photomicrograph 29_03, reflected light, oil immersion, width of field 0.7 mm.

4 – Same sample as Fig. 3. Pyrite framboids in groundmass of lense-shaped aggregates of szomolnokite (szo) and minor amounts of quartz. Photomicrograph 29_04, transmitted and reflected light, oil immersion, width of field 0.7 mm.

5 – Same sample as Fig. 3. Vein-filling coquimbite (coq, yellow) with anhydrite (an, grey-white). Photomicrograph 35_08, transmitted light, width of field 2.8 mm.

6 – Fault-fissure in upper Famennian shales, S of Ain Kahla (loc. 323). Shale fragments replaced by goethite/hematite. Sample 323/25. Photomicrograph 23_11, reflected light, width of field 2.8 mm.

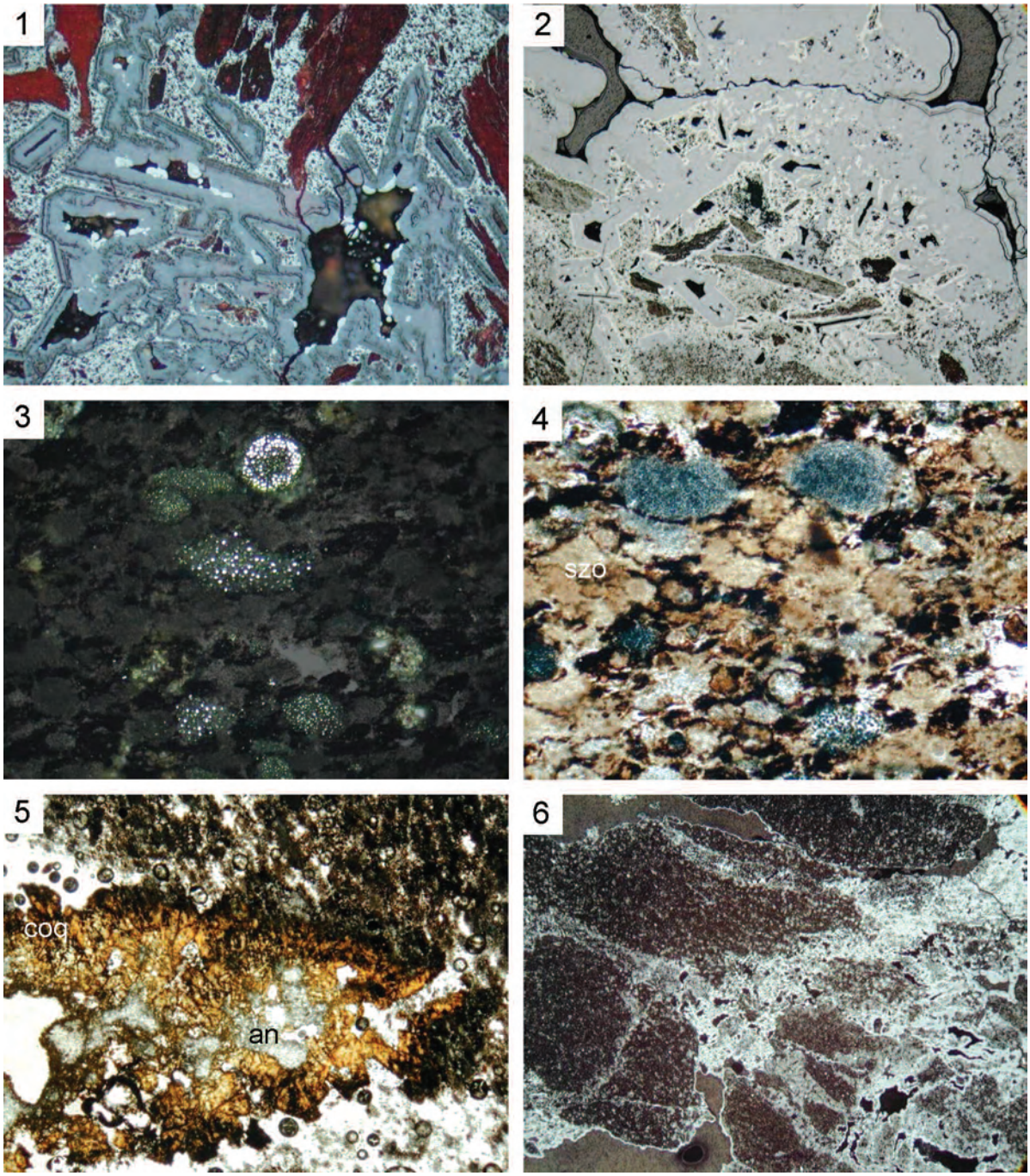
1
2
3
4
SZO
5
cog
an
6